

Non-covalent TMPRSS2 inhibitors identified from virtual screening

Xin Hu*, Jonathan H. Shrimp, Hui Guo, Alexey Zakharov, Sankalp Jain, Paul Shinn, Anton Simeonov, Matthew D. Hall, Min Shen*

National Center for Advancing Translational Sciences (NCATS), National Institutes of Health,
9800 Medical Center Drive, Rockville, MD, 20850, United States

*To whom correspondence should be addressed:

Xin Hu, Ph.D., hux61@mail.nih.gov

Min Shen, Ph.D.; shenmin@mail.nih.gov

Abstract

The SARS-CoV-2 pandemic has prompted researchers to pivot their efforts to finding anti-viral compounds and vaccines. In this study, we focused on the human host cell transmembrane protease serine 2 (TMPRSS2), which plays an important role in the viral life cycle by cleaving the spike protein to initiate membrane fusion. TMPRSS2 is an attractive target and has received significant attention for the development of drugs against SARS and MERS. Starting with comparative structural modeling and binding model analysis, we developed an efficient pharmacophore-based approach and applied in a large-scale *in silico* database screening for small molecule inhibitors against TMPRSS2. A number of novel inhibitors were identified, providing starting points for further development of drug candidates for the treatment of COVID-19.

Keywords: SARS-CoV-2, COVID-19, TMPRSS2, pharmacophore model, virtual screening

Introduction

Severe acute respiratory syndrome coronavirus 2 (SARS-CoV-2) is the virus responsible for the ongoing coronavirus disease 2019 (COVID-19) pandemic.¹ It is a novel betacoronavirus from the same family as SARS-CoV and Middle East respiratory syndrome (MERS).² SARS-CoV-2 produces clinical symptoms that include fever, dry cough, sore throat, dyspnea, headache, pneumonia with potentially progressive respiratory failure owing to alveolar damage, and even death.³ SARS-CoV-2 is a global pandemic with millions of documented infections worldwide by SARS-CoV-2, and over 1 million deaths reported by World Health Organization (WHO). Since no antiviral drug or vaccine existed to treat or prevent SARS-CoV-2, potential therapeutic strategies that are currently being evaluated predominantly stem from previous experience with treating SARS-CoV, MERS-CoV, and other emerging viruses.⁴⁻⁶ Most nations are primarily making efforts to prevent the further spreading of this potentially deadly virus by implementing preventive and control strategies.

A number of processes are considered essential to the viral lifecycle and therefore provide a significant number of targets for inhibiting viral replication. The screening of anti-COVID-19 drugs by using the clinical and approved compounds can greatly shorten the research and development cycle. Some screening campaigns of approved drug libraries and pharmacologically active molecules have been conducted for the discovery of SARS-CoV-2 inhibitors. Antiparasitic drugs like chloroquine and its derivative hydroxychloroquine have shown antiviral activity against SARS-CoV-2 in an in vitro cytopathic assay and had an Emergency Use Authorization awarded and rescinded by the US FDA.^{7, 8} The broad-spectrum antibacterial macrolide azithromycin also has significant antiviral properties, and it decreased the coronavirus infection in cell culture.⁹ The antiviral lopinavir, a protease inhibitor, has also shown inhibitory activity of SARS-CoV-2 infection in Vero E6 cells.¹⁰ The experimental drug remdesivir, a nucleoside analog, originally developed against other viruses, has been approved by the FDA as treatment for COVID-19.¹¹ Despite numerous biochemical and cell-based drug repurposing screening of drug compound libraries that have identified a number of potent antivirals targeting various stages of the viral life cycle the molecular basis of these inhibitors on SARS-CoV-2 and functional studies have generally not been elucidated.

Previous basic and clinical research on coronaviruses has led to the identification of many potential drug targets and determination of their X-ray crystal structures. Structure-based drug design by virtual screening and molecular docking studies has become a valuable primary step in the identification of novel lead molecules for the potential treatment of COVID-19.¹² Cell entry of coronaviruses depends on binding of the viral spike (S) proteins to human cellular receptors and on S protein priming by host cell proteases. It has been demonstrated that SARS-CoV-2 uses the human host cell angiotensin-converting enzyme 2 (ACE2) as the entry receptor and the transmembrane protease serine 2 (TMPRSS2) for S protein priming. Human cellular receptors and proteases critical for viral entry and membrane fusion are now candidate therapeutic targets.¹³ TMPRSS2 has an extracellular protease domain capable of cleaving a spike protein domain to initiate membrane fusion. Considering the vital role played by TMPRSS2 in the viral life cycle, this protease has received significant attention to be used as a potential target to inhibit viral entry into host cells.

In this study, we performed a comprehensive structural modeling and binding site analysis of the serine protease TMPRSS2, followed by a structure-based virtual screening against NCATS library consisting of up to 200,000 drug-like compounds designed from diverse chemical space. After an extensive post-docking analysis in combination with clustering analysis and visual inspection, 350 compounds were selected for experimental validation based on their binding free energy, consensus docking score, and binding interactions with key residues surrounding the active site. The selected hits were evaluated in the TMPRSS2 biochemical assay as well as a fluorescence counter assay.¹⁴ A number of novel and non-covalent inhibitors were identified, providing a starting point for further development of therapeutic drug candidates for COVID-19.

Materials and methods

Inhibitors and homology modeling of TMPRSS2

Three TMPRSS2 inhibitors nafamostat, camostat, and gabexate were used in this study. The activities of these inhibitors against TMPRSS2 have been confirmed in our recent report, with IC₅₀ of 0.27 nM, 6.2 nM, and 130 nM, respectively.¹⁴ The homology model of TMPRSS2 was built using the threading program I-TASSER.¹⁵ The transmembrane trypsin-like serine protease

hepsin (also known as TMPRSS1) which shares 43% of sequence identity with TMPRSS2, was used as the template structure (PDB code 1Z8G).¹⁶

Molecular docking and MD simulations

The structural models of TMPRSS2 was prepared using the Molecular Operating Environment (MOE) program.¹⁷ Consensus docking studies of small molecule inhibitors (camostat and nafamostat) to TMPRSS2 were performed using MOE Dock and AutoDock Vina.¹⁸ The ligand induced fit docking protocol in MOE Dock was applied and binding affinity was evaluated using the GBVI/WSA score. The default parameters in AutoDock Vina were used with a grid box defined at the center of bound ligand by 20 x 20 x 20 Å to encompass the entire active site of the protein. The top-ranked 10 poses from each docking were extracted for consensus analysis.

MD simulations of protein-inhibitor binding complexes were conducted using the AMBER18 package.¹⁹ The simulated system in explicit solvate was first subjected to a gradual temperature increase from 0 K to 300 K over 100 ps, and then equilibrated for 500 ps at 300 K, followed by a production run of 20 ns. Trajectory analysis and binding free energy calculations were performed using the cpptraj module in the AmberTools18.¹⁹

Pharmacophore-based virtual screening

A stepwise virtual screening (VS) protocol combining ligand- and structure-based approach was employed to screen the NCATS's in-house screening libraries consisting of nearly 200,000 drug-like compounds.²⁰ A pharmacophore model was derived from the predicted binding interactions of TMPRSS2 with inhibitors camostat, nafamostat, and gabexate. Two ligand-based approaches were used in the first step of the database search. The pharmacophore-based search was conducted using MOE, and the 3D shape-based mapping was conducted using ROCS.²¹ A total of 20,000 hits were extracted, followed by docking to the active site of TMPRSS2 using MOE dock and AutoDock Vina with default parameters.¹⁸ The top-ranked 2000 compounds from each docking were retained for consensus scoring and binding mode analysis. Structural clustering was performed using MOE. All compounds from each cluster and singletons were visually inspected. Finally, ~350 compounds were selected based on: 1) structural representative of each cluster, 2) predicted binding energy, 3) H-bond interaction with key residues at each binding site, 4)

promiscuous compounds with potential undesirable functionalities and PAINS alert were generally discarded.

TMPRSS2 biochemical assay

A TMPRSS2 biochemical assay has been developed to evaluate the activity of compounds against TMPRSS2.¹⁴ The assay was performed according to the assay protocol: to a 1536-well black plate was added Boc-Gln-Ala-Arg-AMC substrate (20 nL) and test compound (20 nL in DMSO) using an ECHO 655 acoustic dispenser (LabCyte). To that was dispensed TMPRSS2 (150 nL) in assay buffer (50 mM Tris pH 8, 150 mM NaCl, 0.01% Tween20) using a BioRAPTR (Beckman Coulter) to give a total assay volume of 5 μ L. Following 1 h incubation at room temperature, fluorescence was measured using the PHERAstar with excitation at 340 nm and emission at 440 nm.

Fluorescence counter assay

This counter-assay was performed as described previously.¹⁴ To a 1536-well black plate (Corning Cat #3724) was added 7-amino-4-methylcoumarin (20 nL) and inhibitor or DMSO (20 nL) using an ECHO 655 acoustic dispenser (LabCyte). To that was added assay buffer (50 mM Tris pH 8, 150 mM NaCl, 0.01% Tween20) to give a total reaction volume of 5 μ L. Detection was done using the PHERAstar with excitation: 340 nm and emission: 440 nm. Fluorescence was normalized relative to a negative control 7-amino-4-methylcoumarine. An inhibitor causing fluorescence quenching would be identified as having a concentration-dependent decrease on AMC fluorescence.

Results

Binding interaction of TMPRSS2 inhibitor

TMPRSS2 shares 43% of sequence identity with the transmembrane trypsin-like serine protease hepsin (also known as TMPRSS1, gene *HPN*). The modeled structure of TMPRSS2 generated from I-TASSER had a C-score of -0.10 and TM-score of 0.70 which indicated a good quality modeled structure.¹⁵ Similar to the template hepsin and other trypsin-like proteases,

TMPRSS2 shares a common structural fold with a conserved triad residues Ser441, His296, and Asp345 at the active site for catalytic activity.^{22, 23} An predicted oxyanion hole is formed by Gly439 and Gln438 at the active site for the catalytic process and a highly hydrophilic S1 pocket with a conserved Asp435 which is essential for substrate and inhibitor binding.

The predicted binding models of camostat, nafamostat, and gabexate to the active site of TMPRSS2 are shown in **Figure 1**. The three small molecule inhibitors adopted a similar binding mode at the active site of TMPRSS2. While the ester group of the guanidinobenzonate moiety of camostat and nafamostat binds at the triad catalytic site interacting with Ser441 and Gln438, the guanidinium head points into the S1 pocket forming H-bonding and ion interactions with Asp435. The same binding models have been reported by Hempel *et al*, showing that the ester group resembled the substrate peptide bond by forming a covalent bond to the catalytic Ser441, and the high potency of nafamostat can be explained from a greater stability of its Michaelis complex.²⁴ Gabexate binds in a similar manner with the essential guanidinium head interacting with Asp435 in the S1 pocket and the ester group forming hydrogen bonds with Ser441 and Gln438, whereas the benzoic ester group binds to the hydrophobic pocket on the opposite site and forms H-bonding interaction with Glu299.

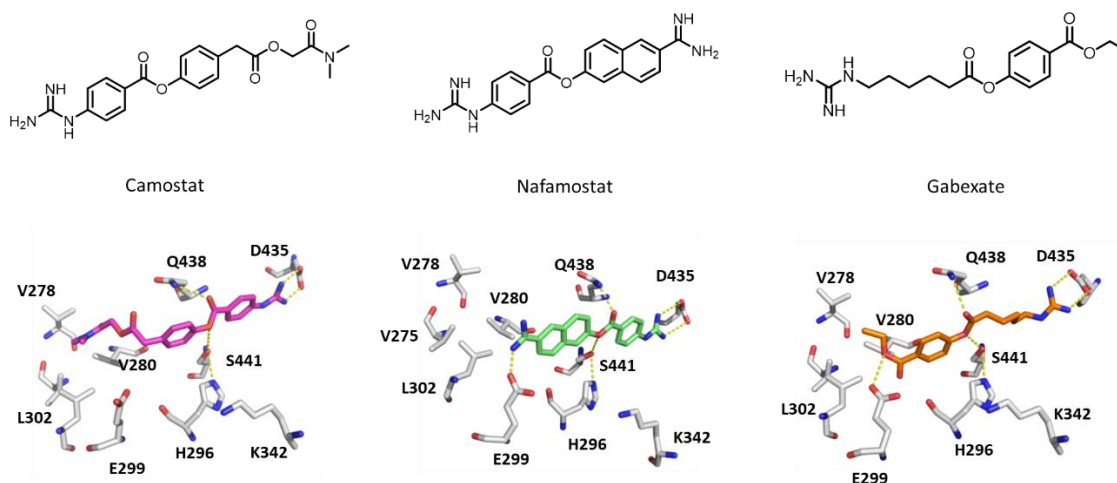


Figure 1. Known TMPRSS2 inhibitors and predicted binding models at the active site of TMPRSS2.

To gain insight into the binding interactions of these inhibitors with TMPRSS2, we performed MD simulations of the inhibitor-bound complexes as compared to the protein in the apo state (**Figure 2A**). The loops surrounding the active site exhibited greater dynamics in the apo form but were significantly stabilized in a closed conformation in the inhibitor binding complex. The hydrogen bonds between the ester group and residues Ser441 and Gln438 at the catalytic site remained stable in the nafamostat and camostat binding complex over the time course of 50-ns simulations, but less stably in the binding complex of gabexate. This may explain the 20-fold weaker activity of gabexate as compared to camostat. Residue Glu299 was found to be highly flexible in the apo protein and preferably interacted with Lys342 in the S2 pocket. This residue is located in the middle of the active site adjacent to the catalytic triad and hydrophobic pocket, which likely plays an important role in facilitating the substrate recognition as well as inhibitor binding.

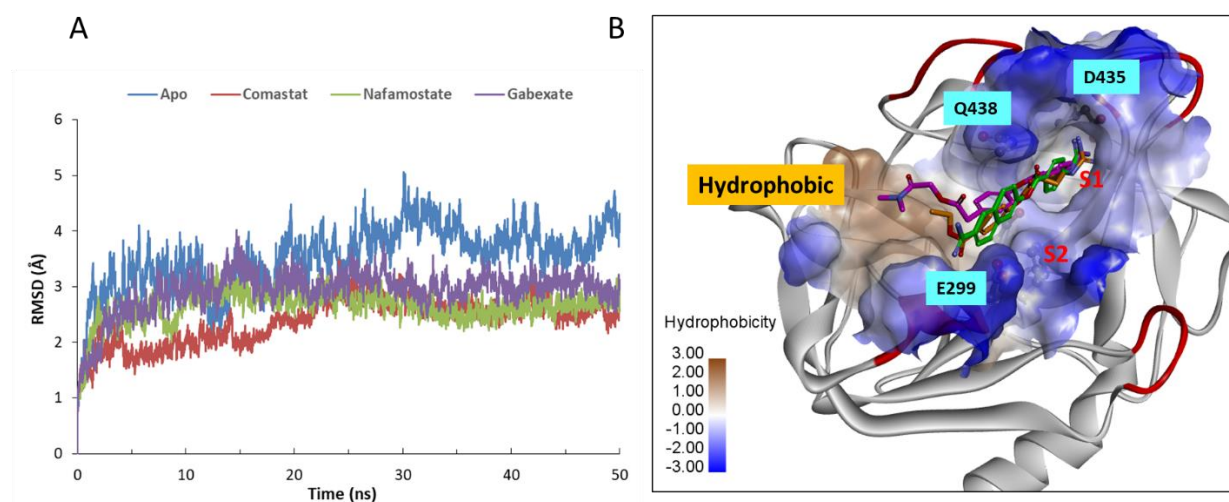


Figure 2. (A) MD simulations of TMPRSS2 in the apo and inhibitor-bound complexes. (B) Inhibitors camostat (magenta), nafamostat (green) and gabexate (dark yellow) bound at the active site of TMPRSS2. The protein surface is rendered in color of hydrophobicity. Dynamics loops surrounding the active site are shown in red. Key residues and the hydrophobic pocket used in pharmacophore model are labeled.

Pharmacophore-based virtual screening

Based on the binding model analysis we developed a pharmacophore model and applied it in virtual screening for novel inhibitors of TMPRSS2. Four pharmacophores were derived from the predicted binding interaction of the three inhibitors (**Figure 2B**). Two structural elements appear

to be essential for binding: one is the interaction of guanidinium head with Asp435 in the S1 pocket; the other is the core interaction at the catalytic site with the triad residues and Gln438 to the oxyanion hole. On the opposite side, the hydrophobic pocket formed by Val275, Val280, and Leu302 serves as an extended region to accommodate variable groups for enhanced binding affinity, while the adjacent Glu299 provides a key interaction to position the inhibitor into these binding pockets.

Virtual screening was performed in a stepwise way combined with pharmacophore-based searching, 3D-shape-based mapping, and structure-based docking (**Figure 3**). An in-house collection of nearly 200,000 drug-like compounds were virtually screened. To prioritize the hits generated from docking, several post-processing approaches were applied including docking pose analysis, structural clustering, re-scoring, and promiscuity filtering. Ultimately, ~350 compounds were selected based on the predicted binding energy, key interactions within the catalytic triad and functional head in the S1 pocket, the novelty of scaffold and chemotypes. Promiscuous compounds (i.e., those shown to have high hit rates across HTS assays experimentally screened at NCATS) with potential undesirable functionalities and PAINS alerts were generally discarded.

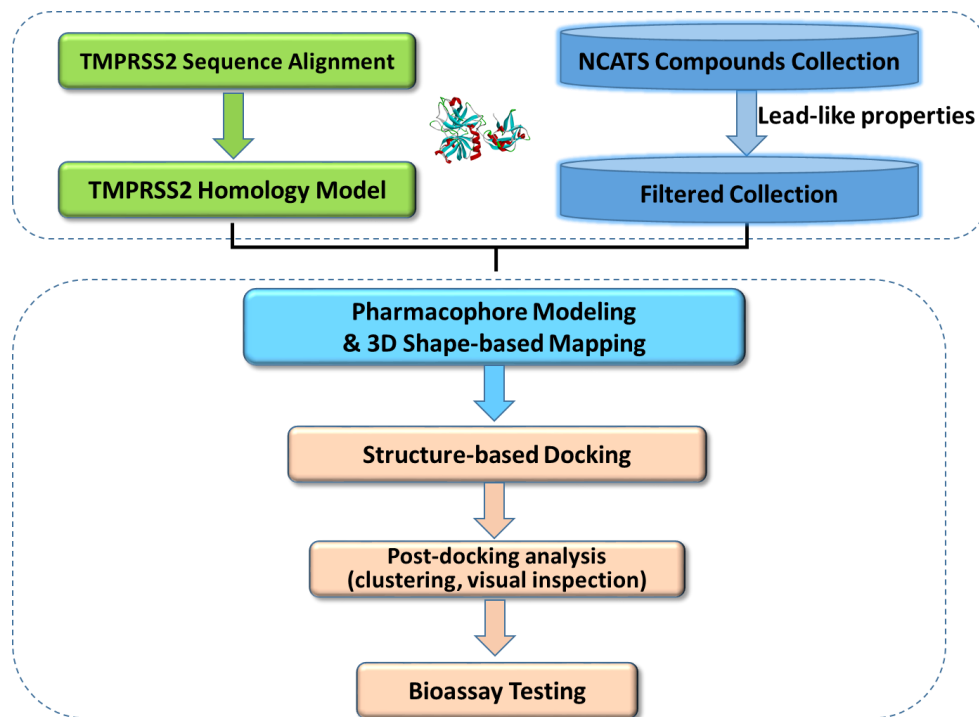


Figure 3. Flowchart of virtual screening.

TMPRSS2 inhibitors identified from VS

All selected compounds were evaluated in the TMPRSS2 enzymatic assay, a fluorogenic biochemical assay we reported recently.¹⁴ A counter assay was conducted to detect all positive compounds with fluorescence quenching properties that suppress the fluorescence signal generated by the protease activity on the fluorogenic substrate. The three inhibitors camostat, nafamostat and gabexate were also tested in the assay as positive controls, and all showed the same inhibitory activities as previously reported.¹⁴ Of 350 compounds tested, 14 hits showed inhibition with activity efficacy greater than 50% and IC₅₀ ranging from 2 μM to 30 μM (**Table S1**). The best hit of otamixaban (NCGC00378763) had an IC₅₀ of 2.2 μM and 100% inhibition activity, while the other two full inhibition hits UKI-1 (NCGC00522442) and NCGC00386945 showed IC₅₀ of 3.5 μM and 10.0 μM, respectively. All three inhibitors possess a benzoamidinium head group. Other less efficacious and weak inhibitors are more structurally diverse with a different functional group bound to the S1 pocket (**Figure 4 and Figure 5**).

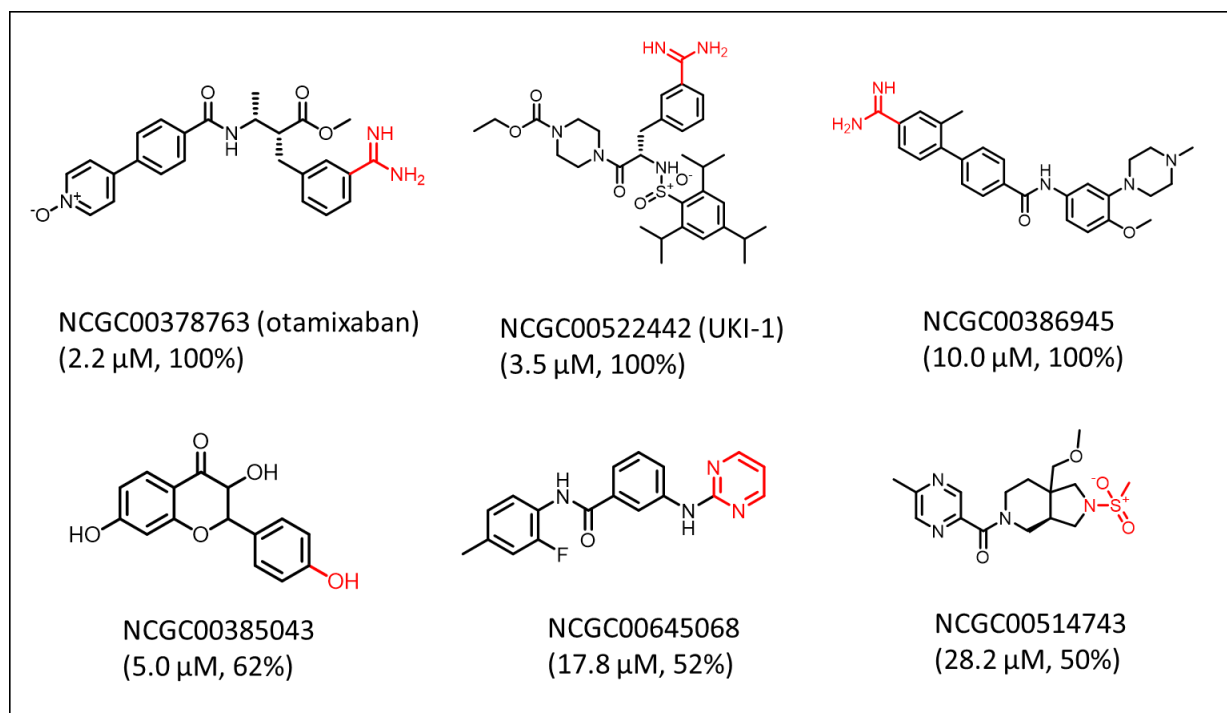


Figure 4. TMPRSS2 inhibitors identified from VS. The head group bound in the S1 pocket is colored in red.

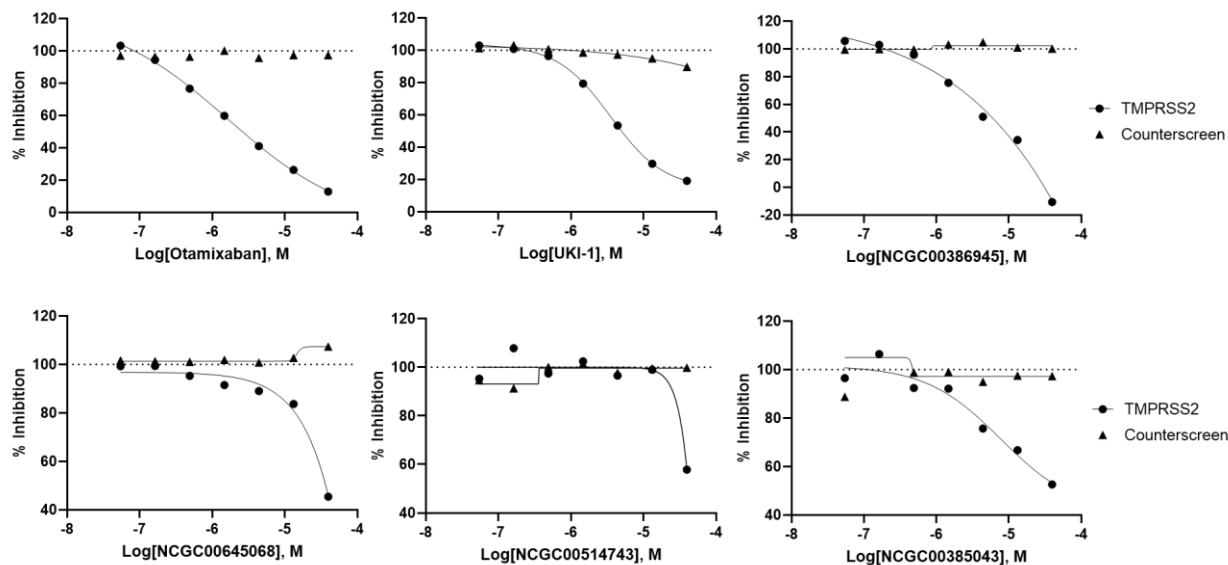


Figure 5. Confirmed activities in the TMPRSS2 enzyme assay and counter screen.

To probe the binding mechanism of the identified inhibitors, we compared the binding models of these compounds bound at the active site of TMPRSS2 with camostat (**Figure 6**). As expected, the three full inhibition compounds utilized the benzoamidinium group to engage the key interaction with Asp435 in the S1 pocket, while another functional group was accommodated to the hydrophobic pocket by forming H-bonding or ion interaction with Glu299. MD simulations showed that these inhibitors bound stably at the active site of TMPRSS2, similar to the observed simulation with camostat and nafamostat. Different from these covalent inhibitors, otamixaban and NCGC00386945 have an amide group to predominately interact with the catalytic triad residues through non-covalent hydrogen bond interactions. Notably, UKI-1 occupied an additional binding interaction at the S2 pocket. However, the binding interactions of the bulky triisopropyl phenylsulfonyl group appeared not to be optimized for TMPRSS2. As shown in the predicted binding model, TMPRSS2 possesses several polar residues including a unique Lys342 at this site, which makes it possible to further optimize the binding interactions to improve the potency and selectivity to TMPRSS2.

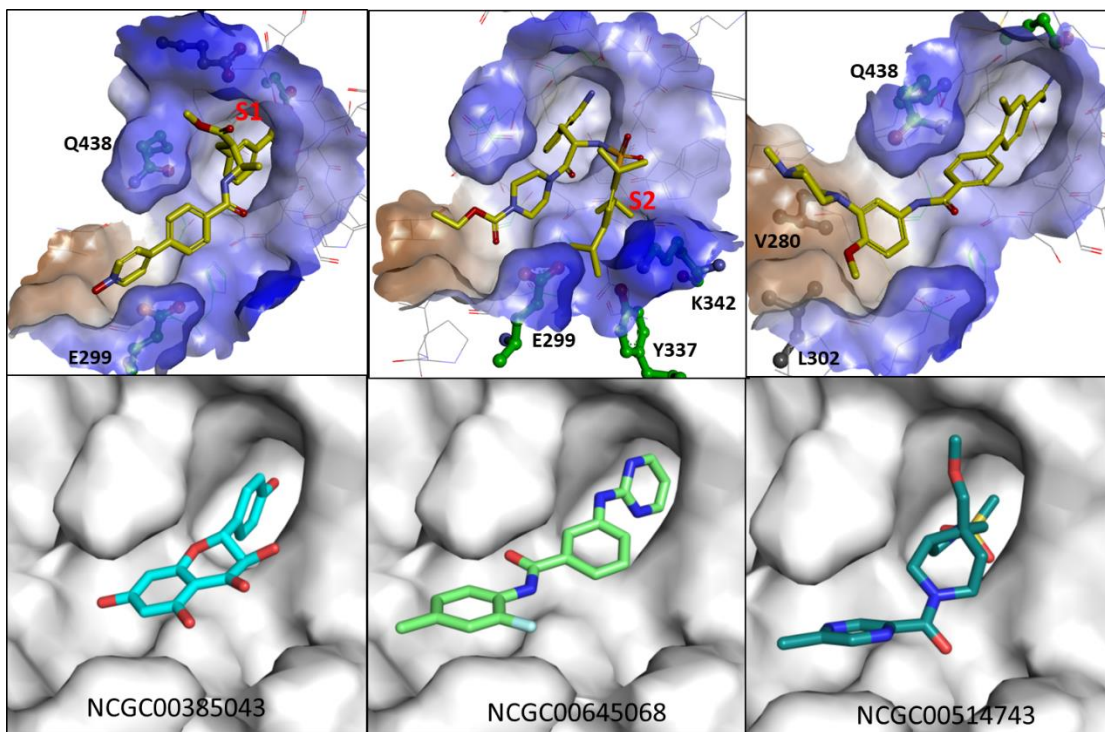


Figure 6. Predicted binding models of non-covalent inhibitors bound at the active site of TMPRSS2. (up panel) Three full inhibitory inhibitors otamixaban, UKI-1, and NCGC00386945. Protein surface is shown in hydrophobic representation. (low panel) Three partial inhibition hits bound in the catalytic binding site. The protein surface is shown in white.

DISCUSSION

The host serine protease TMPRSS2 is an attractive target for drug development against SARS-CoV-2. However, unlike viral proteases such as 3Clpro which has been extensively investigated recently and a large number of inhibitors have been reported,²⁵ TMPRSS2 has been less studied and very few compounds have been evaluated in drug re-purposing screening. The enzyme is membrane associated, making it more challenging to express recombinant protein and study in vitro. Although camostat and nafamostat have progressed into clinical trials for the treatment of COVID-19, these inhibitors also show potent activity against many other trypsin-like serine proteases such as the plasma trypsin-like proteases, plasmin and FXIa.¹⁴ Therefore, there is an

unmet need for novel and selective candidates of TMPRSS2 inhibition for further drug development.

We began the virtual screening campaign by iteratively searching and docking nearly 200,000 compounds to the active site of TMPRSS2, followed by testing 350 compounds in the TMPRSS2 biochemical assay. Several interesting inhibitors were identified. Otamixaban is an experimental anticoagulant direct factor Xa inhibitor that was investigated for the treatment of acute coronary syndrome but its development was terminated in a Phase III clinical trial due to poor performance.²⁶ Otamixaban displayed efficient inhibitory activity with an IC₅₀ of 2.2 μM against TMPRSS2, suggesting this to be a good candidate to further evaluate in the viral inhibition assay for drug re-purposing. UKI-1 is a selective inhibitor of trypsin and uPA.²⁷ While it displayed potent inhibition against TMPRSS2 at single digit micromole, it is interesting to further explore the binding interactions of this series of compounds bound at the S2 hydrophobic pocket to improve the potency and selectivity to TMPRSS2. NCGC00386945 is a novel chemotype that was originally developed as a selective 5-HT1D antagonist.²⁸ An analog of inhibitor NCGC00386945 with an oxadiazol head (NCGC00386477) showed less efficacy and a 3-fold decrease in potency, reiterating a key role of the functional group for effective binding and inhibition against the serine protease.

A number of hits identified from the VS also showed inhibition in the TMPRSS2 assay with 50%-70% maximal efficacy. These compounds represent a diversity of structures that were not reported as serine protease inhibitors. The quinol-like inhibitor NCGC00385043 is particularly interesting as a number of analog compounds and drug molecules showed similar inhibition against TMPRSS2, suggesting that it is a promising class of compounds for further evaluation. Unlike the other full inhibition hits, these compounds bind predominately at the catalytic site of TMPRSS2 by catching H-binding interactions with the triad residue. While they lack a typical warhead group in the S1 pocket, the small molecule fragments are more structurally diverse and drug-like, providing a variety of appealing scaffolds that may serve as starting points for the development of potent inhibitors against TMPRSS2.

It is worth mentioning that the inhibitors identified from this VS campaign are expected to be non-covalent protease inhibitors. This is in part due to the docking-based approach which is not capable of identifying a covalent binder. On the other hand, we were inclined to deprioritize the traditional covalent protease inhibitors in the VS in order to identify novel and non-covalent chemotypes. Compared to the covalent inhibitors such as camostat and nafamostat with a reactive functional group to the highly conserved catalytic site,²⁹ the non-covalent inhibitors are less chemically and metabolically reactive, therefore, are more advantageous and attractive in the design of selective inhibitors. A number of non-covalent inhibitors of thrombin and factor Xa have been reported.³⁰ As revealed from the binding models of these identified inhibitors, TMPRSS2 showed different structural features and binding specificity at the distal hydrophobic pocket, which makes it a promising target for structure-based design and chemistry lead optimization to achieve selectivity and drug-like properties as drug candidates for the treatment of COVID-19.

ACKNOWLEDGMENTS

This work was supported by the Intramural Research Programs of the National Center for Advancing Translational Sciences, National Institutes of Health.

REFERENCES

1. Lai, C. C.; Shih, T. P.; Ko, W. C.; Tang, H. J.; Hsueh, P. R., Severe acute respiratory syndrome coronavirus 2 (SARS-CoV-2) and coronavirus disease-2019 (COVID-19): The epidemic and the challenges. *Int J Antimicrob Agents* **2020**, *55* (3), 105924.
2. Lu, R.; Zhao, X.; Li, J.; Niu, P.; Yang, B.; Wu, H.; Wang, W.; Song, H.; Huang, B.; Zhu, N.; Bi, Y.; Ma, X.; Zhan, F.; Wang, L.; Hu, T.; Zhou, H.; Hu, Z.; Zhou, W.; Zhao, L.; Chen, J.; Meng, Y.; Wang, J.; Lin, Y.; Yuan, J.; Xie, Z.; Ma, J.; Liu, W. J.; Wang, D.; Xu, W.; Holmes, E. C.; Gao, G. F.; Wu, G.; Chen, W.; Shi, W.; Tan, W., Genomic characterisation and epidemiology of 2019 novel coronavirus: implications for virus origins and receptor binding. *Lancet* **2020**, *395* (10224), 565-574.
3. Zhou, P.; Yang, X. L.; Wang, X. G.; Hu, B.; Zhang, L.; Zhang, W.; Si, H. R.; Zhu, Y.; Li, B.; Huang, C. L.; Chen, H. D.; Chen, J.; Luo, Y.; Guo, H.; Jiang, R. D.; Liu, M. Q.; Chen, Y.; Shen, X. R.; Wang, X.; Zheng, X. S.; Zhao, K.; Chen, Q. J.; Deng, F.; Liu, L. L.; Yan, B.; Zhan, F. X.; Wang, Y. Y.; Xiao, G. F.; Shi, Z. L., A pneumonia outbreak associated with a new coronavirus of probable bat origin. *Nature* **2020**, *579* (7798), 270-273.
4. Lu, H., Drug treatment options for the 2019-new coronavirus (2019-nCoV). *Biosci Trends* **2020**, *14* (1), 69-71.
5. Sheahan, T. P.; Sims, A. C.; Leist, S. R.; Schafer, A.; Won, J.; Brown, A. J.; Montgomery, S. A.; Hogg, A.; Babusis, D.; Clarke, M. O.; Spahn, J. E.; Bauer, L.; Sellers, S.; Porter, D.; Feng, J. Y.; Cihlar, T.; Jordan, R.; Denison, M. R.; Baric, R. S., Comparative

therapeutic efficacy of remdesivir and combination lopinavir, ritonavir, and interferon beta against MERS-CoV. *Nat Commun* **2020**, *11* (1), 222.

6. Pillaiyar, T.; Meenakshisundaram, S.; Manickam, M., Recent discovery and development of inhibitors targeting coronaviruses. *Drug Discov Today* **2020**, *25* (4), 668-688.

7. Wang, M.; Cao, R.; Zhang, L.; Yang, X.; Liu, J.; Xu, M.; Shi, Z.; Hu, Z.; Zhong, W.; Xiao, G., Remdesivir and chloroquine effectively inhibit the recently emerged novel coronavirus (2019-nCoV) in vitro. *Cell Res* **2020**, *30* (3), 269-271.

8. Liu, J.; Cao, R.; Xu, M.; Wang, X.; Zhang, H.; Hu, H.; Li, Y.; Hu, Z.; Zhong, W.; Wang, M., Hydroxychloroquine, a less toxic derivative of chloroquine, is effective in inhibiting SARS-CoV-2 infection in vitro. *Cell Discov* **2020**, *6*, 16.

9. Touret, F.; Gilles, M.; Barral, K.; Nougairede, A.; van Helden, J.; Decroly, E.; de Lamballerie, X.; Coutard, B., In vitro screening of a FDA approved chemical library reveals potential inhibitors of SARS-CoV-2 replication. *Sci Rep* **2020**, *10* (1), 13093.

10. Choy, K. T.; Wong, A. Y.; Kaewpreedee, P.; Sia, S. F.; Chen, D.; Hui, K. P. Y.; Chu, D. K. W.; Chan, M. C. W.; Cheung, P. P.; Huang, X.; Peiris, M.; Yen, H. L., Remdesivir, lopinavir, emetine, and homoharringtonine inhibit SARS-CoV-2 replication in vitro. *Antiviral Res* **2020**, *178*, 104786.

11. Shyr, Z. A.; Gorshkov, K.; Chen, C. Z.; Zheng, W., Drug Discovery Strategies for SARS-CoV-2. *J Pharmacol Exp Ther* **2020**, *375* (1), 127-138.

12. Naik, B.; Gupta, N.; Ojha, R.; Singh, S.; Prajapati, V. K.; Prusty, D., High throughput virtual screening reveals SARS-CoV-2 multi-target binding natural compounds to lead instant therapy for COVID-19 treatment. *Int J Biol Macromol* **2020**, *160*, 1-17.

13. Hoffmann, M.; Kleine-Weber, H.; Schroeder, S.; Kruger, N.; Herrler, T.; Erichsen, S.; Schiergens, T. S.; Herrler, G.; Wu, N. H.; Nitsche, A.; Muller, M. A.; Drosten, C.; Pohlmann, S., SARS-CoV-2 Cell Entry Depends on ACE2 and TMPRSS2 and Is Blocked by a Clinically Proven Protease Inhibitor. *Cell* **2020**, *181* (2), 271-280 e8.

14. Shrimp, J. H.; Kales, S. C.; Sanderson, P. E.; Simeonov, A.; Shen, M.; Hall, M. D., An Enzymatic TMPRSS2 Assay for Assessment of Clinical Candidates and Discovery of Inhibitors as Potential Treatment of COVID-19. *bioRxiv* **2020**.

15. Roy, A.; Kucukural, A.; Zhang, Y., I-TASSER: a unified platform for automated protein structure and function prediction. *Nat Protoc* **2010**, *5* (4), 725-38.

16. Herter, S.; Piper, D. E.; Aaron, W.; Gabriele, T.; Cutler, G.; Cao, P.; Bhatt, A. S.; Choe, Y.; Craik, C. S.; Walker, N.; Meininger, D.; Hoey, T.; Austin, R. J., Hepatocyte growth factor is a preferred in vitro substrate for human hepsin, a membrane-anchored serine protease implicated in prostate and ovarian cancers. *Biochem J* **2005**, *390* (Pt 1), 125-36.

17. *Molecular Operating Environment (MOE) 2019.01*. Chemical Computing Group ULC, Montreal, QC, Canada.

18. Trott, O.; Olson, A. J., AutoDock Vina: improving the speed and accuracy of docking with a new scoring function, efficient optimization, and multithreading. *J Comput Chem* **2010**, *31* (2), 455-61.

19. Case, D. A.; Ben-Shalom, I. Y.; Brozell, S. R.; D.S., C.; T.E., C. I.; Cruzeiro, V. W. D.; Darden, T. A.; Duke, R. E.; Ghoreishi, D.; Simmerling CL; Wang J; Luo R; Merz KM; Wang B; Pearlman DA; Crowley M; Tsui V; Gohlke H; Mongan J; Hornak V; Cui G; Beroza P; Schafmeister C; Walker, R. C.; Wei, H.; Wolf, R. M.; Wu, X.; Xiao, L.; York, D. M.; Kollman, P. A., *AMBER18*. University of California, San Francisco: 2018.

20. Hu, X.; Zhang, Y. Q.; Lee, O. W.; Liu, L.; Tang, M.; Lai, K.; Boxer, M. B.; Hall, M. D.; Shen, M., Discovery of novel inhibitors of human galactokinase by virtual screening. *J Comput Aided Mol Des* **2019**, *33* (4), 405-417.
21. Hawkins, P. C.; Skillman, A. G.; Nicholls, A., Comparison of shape-matching and docking as virtual screening tools. *J Med Chem* **2007**, *50* (1), 74-82.
22. Rensi, S.; Altman, R. B.; Liu, T.; Lo, Y. C.; McInnes, G.; Derry, A.; Keys, A., Homology Modeling of TMPRSS2 Yields Candidate Drugs That May Inhibit Entry of SARS-CoV-2 into Human Cells. *ChemRxiv* **2020**.
23. Hedstrom, L., Serine protease mechanism and specificity. *Chem Rev* **2002**, *102* (12), 4501-
24. Hempel, T.; Raich, L.; Olsson, S.; Azouz, N.; Klingler, A.; Rothenberg, M.; Noe, F., Molecular mechanism of SARS-CoV-2 cell entry inhibition via TMPRSS2 by Camostat and Nafamostat mesylate. *bioRxiv* **2020**, doi: <https://doi.org/10.1101/2020.07.21.214098>.
25. Zhu, W.; Xu, M.; Chen, C. Z.; Guo, H.; Shen, M.; Hu, X.; Shinn, P.; Klumpp-Thomas, C.; Michael, S. G.; Zheng, W., Identification of SARS-CoV-2 3CL Protease Inhibitors by a Quantitative High-throughput Screening. *bioRxiv* **2020**.
26. Guertin, K. R.; Choi, Y. M., The discovery of the Factor Xa inhibitor otamixaban: from lead identification to clinical development. *Curr Med Chem* **2007**, *14* (23), 2471-81.
27. Sturzebecher, J.; Vieweg, H.; Steinmetzer, T.; Schweinitz, A.; Stubbs, M. T.; Renatus, M.; Wikstrom, P., 3-Amidinophenylalanine-based inhibitors of urokinase. *Bioorg Med Chem Lett* **1999**, *9* (21), 3147-52.
28. Liao, Y.; Bottcher, H.; Harting, J.; Greiner, H.; van Amsterdam, C.; Cremers, T.; Sundell, S.; Marz, J.; Rautenberg, W.; Wikstrom, H., New selective and potent 5-HT(1B/1D) antagonists: chemistry and pharmacological evaluation of N-piperazinylphenyl biphenylcarboxamides and biphenylsulfonamides. *J Med Chem* **2000**, *43* (3), 517-25.
29. Sun, W.; Zhang, X.; Cummings, M. D.; Albaranzaji, K.; Wu, J.; Wang, M.; Alexander, R.; Zhu, B.; Zhang, Y.; Leonard, J.; Lanter, J.; Lenhard, J., Targeting enteropeptidase with reversible covalent inhibitors to achieve metabolic benefits. *J Pharmacol Exp Ther* **2020**.
30. Sanderson, P. E., Small, noncovalent serine protease inhibitors. *Med Res Rev* **1999**, *19* (2), 179-97.